ISSN 1070-3284, Russian Journal of Coordination Chemistry, 2016, Vol. 42, No. 3, pp. 178–186. © Pleiades Publishing, Ltd., 2016.
Original Russian Text © E.A. Katlenok, A.A. Zolotarev, A.Yu. Ivanov, S.N. Smirnov, R.I. Baichurin, K.P. Balashev, 2016, published in Koordinatsionnaya Khimiya, 2016, Vol. 42, No. 3, pp. 156–163.

Complexes of Ir(III) and Pt(II) with Cyclometallated 2-Phenylbenzothiazole and Chelating Diethyldithiocarbamate and O-Ethyldithiocarbonate Ions: Structures and Optical and Electrochemical Properties

E. A. Katlenok[a], A. A. Zolotarev[b], A. Yu. Ivanov[b], S. N. Smirnov[b], R. I. Baichurin[a], and K. P. Balashev[a, *]

[a] *Gertsen Russian State Pedagogical University, St. Petersburg, Russia*

[b] *St. Petersburg State University, St. Petersburg, Russia*

**e-mail: k_balashev@mail.ru*

Received April 21, 2015

Abstract—It is shown by X-ray diffraction analysis, IR spectroscopy, and ^{1}H, $^{13}C\{1H\}$, and ^{195}Pt NMR spectroscopy that the Pt(II) and octahedral Ir(III) complexes with metallated 2-phenylbenzothiazole and chelating diethyldithiocarbamate and O-ethyldithiocarbonate ions have the square and *cis*-C,C structure, respectively. The highest occupied and lowest unoccupied molecular orbitals of the complexes determining their long-wavelength absorption, phosphorescence, and one-electron oxidation and reduction are assigned to those predominantly localized on the mixed $p(S)/d(M)$ and π^* orbitals of the metallated ligand. The cathodic shift of the oxidation voltammogram and the bathochromic phosphorescence shift of the Pt(II) complex with the O-ethyldithiocarbonate ion are attributed to the enhanced donor–acceptor interaction of the donor S atoms of the ligand with Pt(II). The structural data are deposited with the Cambridge Crystallographic Data Centre (CIF files CCDC nos. 1058768 (**Ia**) and 1058767 (**IIb**)).

DOI: 10.1134/S1070328416030039

INTRODUCTION

Phosphorescence at room temperature and one-electron electrochemical processes of outer-sphere electron transfer in the cyclometallated Ir(III) and Pt(II) complexes induce increased interest in these compounds [1] due to wide prospects of their use in organic light diodes [2], photocatalysts of hydrogen evolution [3], luminescent labels of biosystems [4], and optical and electrochemical chemisensors [5]. These complexes contain chelating ligands along with cyclometallated ligands, which significantly extends possibilities of the targeted change in the nature of their highest occupied and lowest unoccupied molecular orbitals (HOMO and LUMO, respectively) responsible for the optical and electrochemical properties [6].

The results of X-ray diffraction analysis, IR spectroscopy, ^{1}H, $^{13}C\{1H\}$, and ^{195} Pt NMR spectroscopy, electronic absorption and emission spectroscopy, and voltammetry are presented in this work for the complexes $[Ir(Pbt)_2Dtc]$ (**Ia**), $[Ir(Pbt)_2Exn]$ (**Ib**), [Pt(Pbt)Dtc] (**IIa**), and [Pt(Pbt)Exn] (**IIb**) (Pbt^- is cyclometallated 2-phenylbenzothiazole, Dtc^- is diethyldithiocarbamate ion, and Exn^- is O-ethyldithiocarbonate ion):

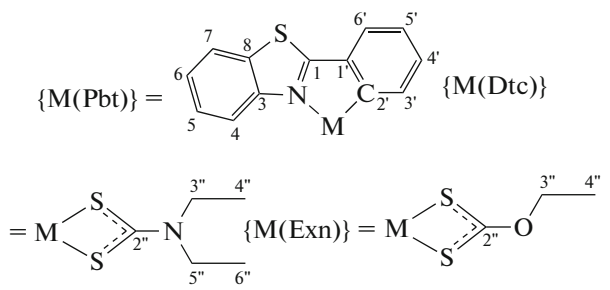

EXPERIMENTAL

Complexes **Ia**, **Ib**, **IIa**, and **IIb** were synthesized using reagent grade reagents and similar procedures (~75% yield). A mixture of $[Pt(Pbt)(\mu\text{-}Cl)]_2$ or $[Ir(Pbt)_2(\mu\text{-}Cl)]_2$ (1 equiv.) [7] and $AgNO_3$ (2 equiv.) in acetonitrile was refluxed until the precipitation of white AgCl. The precipitate was filtered off, and $Na(Dtc) \cdot 3H_2O$ (for **Ia** and **IIa**) or K(Exn) (for **Ib** and **IIb**) (2 equiv.) in methanol was added to the filtrate. The obtained reaction mixture was refluxed until the formation of an orange precipitate, which was washed with methanol and *n*-pentane and dried in air. Single crystals of complexes **Ia** and **IIb** were obtained by the

Table 1. Crystallographic data and refinement parameters for structures $[Ir(Pbt)_2(Dtc)]$ (**Ia**) and [Pt(Pbt)(Exn)] (**IIb**)

Parameter	Value	
	Ia	**IIb**
Empirical formula	$C_{31}H_{26}N_4S_4Ir$	$C_{16}H_{13}NOS_3Pt$
FW	775.00	526.54
Crystal system	Orthorhombic	Monoclinic
Space group	*C*2*cb*	$P2_1/c$
Unit cell parameters:		
a, Å	12.3227(3)	10.0437(3)
b, Å	15.4520(3)	5.68736(17)
c, Å	14.7546(3)	27.6934(9)
β, deg	90.00	90.070(3)
V, Å^{-3}; Z	2809.44(10); 4	1581.91(8); 4
ρ_{calcd}, g/cm^3	1.832	2.211
μ, mm^{-1}	5.080	9.265
F(000)	1524	1000
2θ range, deg	5.05–52.99	7.144–56.00
Index range	$-15 \leqslant h \leqslant 15, -19 \leqslant k \leqslant 19, -18 \leqslant l \leqslant 18$	$-13 \leqslant h \leqslant 11, -4 \leqslant k \leqslant 7, -28 \leqslant l \leqslant 36$
Total number of reflections	13418	9115
Independent reflections (R_{int})	2856 (0.0369)	3788 (0.0578)
GOOF	1.164	1.026
R factors ($F_0 \geqslant 4\sigma F$)	$R_1 = 0.0339$, $wR_2 = 0.0845$	$R_1 = 0.0477$, $wR_2 = 0.1217$
R factors (all data)	$R_1 = 0.0372$, $wR_2 = 0.0871$	$R_1 = 0.0549$, $wR_2 = 0.1277$
ρ_{min}, ρ_{max}, *e*/ Å^{-3}	1.75/–2.60	4.53/–3.19

$R_1 = \Sigma\|F_o| - |F_c\|/\Sigma|F_o|$; $wR_2 = \{\Sigma[w(F_o^2 - F_c^2)^2]/\Sigma[w(F_o^2)^2]\}^{1/2}$; $w = 1/[\sigma^2(F_o^2) + (aP)^2 + bP]$, where $P = (F_o^2 + 2F_c^2)/3$; $s = \{\Sigma[w(F_o^2 - F_c^2)]/(n-p)\}^{1/2}$, *n* is the number of reflections, and *p* is the number of refined parameters.

slow evaporation of solutions of the complexes in dichloromethane.

The X-ray diffraction analyses of complexes **Ia** and **IIb** were carried out at 100 K on an Agilent Technologies Excaliburs Eos single-crystal diffractometer (Resource Center "X-ray Diffraction Research Methods," St. Petersburg State University) equipped with a planar detector of reflected X-ray beams of the CCD type (MoK_α radiation, λ = 0.71073 Å). The crystallographic data and refinement parameters for structures **Ia** and **IIb** are presented in Table 1. The unit cell parameters were refined by the least-squares method. The structures were solved by direct methods and refined using the SHELX program [8] in the OLEX2 program package [9]. An absorption correction was applied in the CrysAlisPro program package [10]. Random disordering of the crystallographic positions N(2) and C(15) of the diethyldithiocarbamate ligand is observed for structure **Ia** (Fig. 1b). The hydrogen atoms were included into the refinement with fixed positional and temperature parameters.

The structural information was deposited with the Cambridge Crystallographic Data Centre (CIF files nos. 1058768 (**Ia**) and 1058767 (**IIb**); deposit@ccdc.cam.ac.uk or http://www.ccdc.cam.ac.uk/data_request/cif).

The ^{1}H, ^{13}C{1H}, dqf-COSY, ^{1}H–^{13}C HMQC, and ^{1}H–^{13}C HMBC NMR spectra of the complexes in $CDCl_3$ solutions were recorded on a Jeol JNM-ECX-400A spectrometer with the working frequencies 399.78 MHz (^{1}H) and 100.53 MHz (^{13}C) of the Center for Collective Use at the Department of Chemistry of

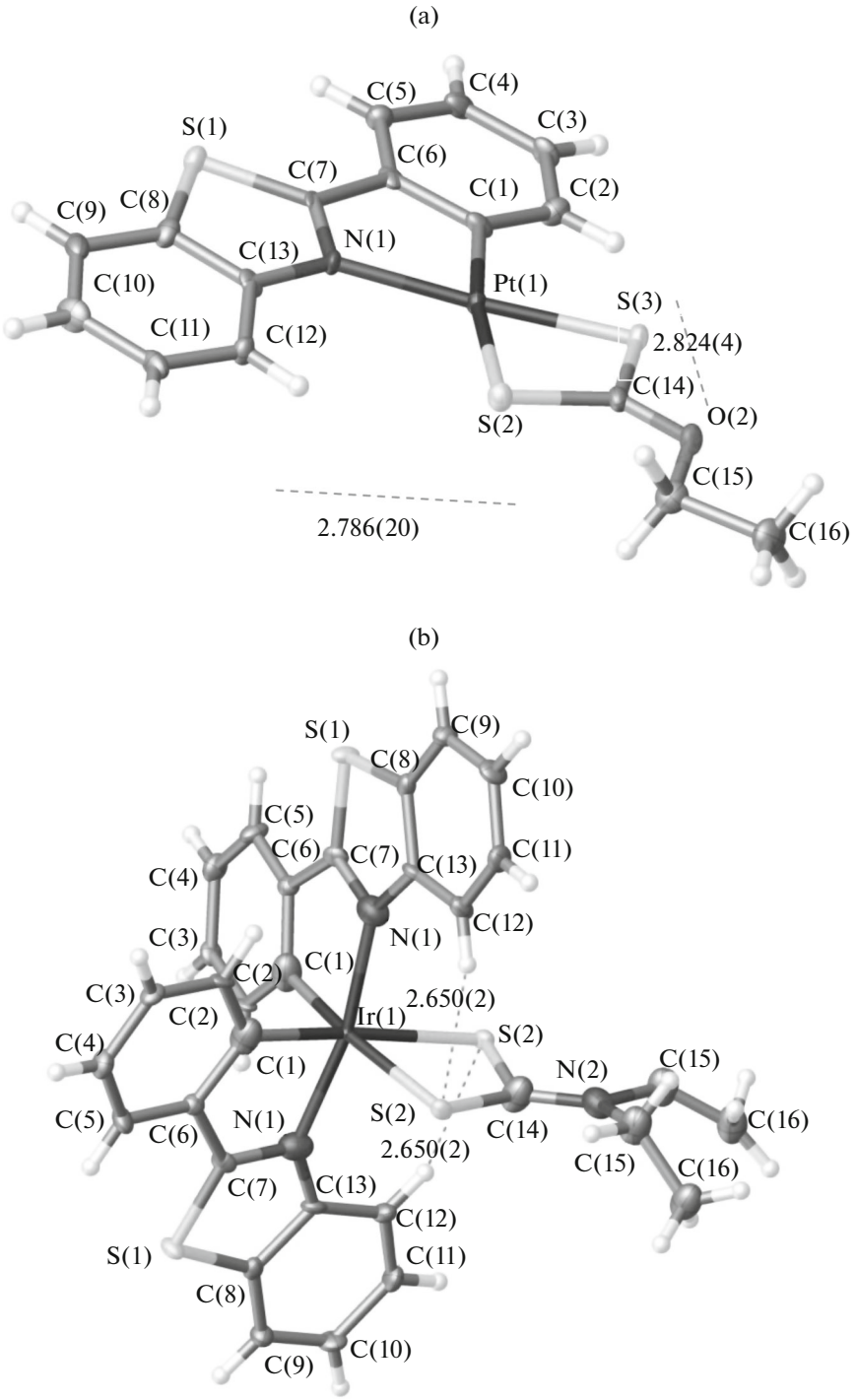

Fig. 1. Molecular structures of complexes (a) **IIb** and (b) **Ia**.

the Gertsen Russian State Pedagogical University. Signals of residual protons of the deuterated solvent were used as internal standards. The ^{195}Pt NMR spectra in a CD_2Cl_2 solution (86.015 MHz) and the selective 1D NOE spectrum in a $CDCl_3$ solution were obtained on a Bruker Avance III 400 spectrometer of the Resource Center "Magnetic Resonance Research Methods" at the St. Petersburg State University.

Diethyldithiocarbamatobis((2-phenyl-3-ido)benzothiazole)iridium (**Ia**). ^{1}H NMR ($CDCl_3$; δ, ppm (*J*, Hz)): for {Ir(Pbt)$_2$}, 9.44 d ($^3J_{HH}$ 8.1; 2H^4), 7.92 d

($^3J_{HH}$ 7.6; 2H^7), 7.67 d ($^3J_{HH}$ 7.5; 2H$^{6'}$), 7.48 m (4H^{5,6}), 6.84 td ($^3J_{HH}$ 7.2, $^4J_{HH}$ 1.4; 2H$^{5'}$), 6.65 td ($^3J_{HH}$ 7.8, $^4J_{HH}$1.4; 2H$^{4'}$), 6.59 d ($^3J_{HH}$ 7.5; 2H$^{3'}$); for {Ir(Dtc)}, 3.97 q ($^3J_{HH}$ 7.0; 2H$^{3''}$), 3.19 q ($^3J_{HH}$ 7.0; 2H$^{5''}$), 1.15 t ($^3J_{HH}$ 7.0; 6H$^{4'', 6''}$). ^{13}C{1H} NMR ($CDCl_3$), δ, ppm: for {Ir(Pbt)$_2$}, 180.0 (2C^1), 156.4 (2C$^{2'}$), 151.6 (2C^3), 141.0 (2C$^{1'}$), 133.9 (2C$^{3'}$), 132.1 (2C^8), 129.8 (2C$^{4'}$), 126.6 (2C^5), 125.7 (2C$^{6'}$), 124.9 (2C^6), 123.0 (2C^4), 122.2 (2C^7), 121.0 (2C$^{5'}$); for {Ir(Dtc)}, 209.9 (C$^{2''}$), 43.2 (2C$^{3'', 5''}$), 12.4 2C$^{4'', 6''}$.

Diethyldithiocarbamatobis((2-phenyl-3-ido)benzothiazole)platinum (**IIa**). ^{1}H NMR ($CDCl_3$; δ, ppm (*J*, Hz)): for {Pt(Pbt)}, 7.90 ddd ($^3J_{HH}$ 8.3, $^4J_{HH}$ 1.0, $^5J_{HH}$ 0.6; H^4), 7.82 ddd ($^3J_{HH}$ 8.0, $^4J_{HH}$ 1.2, $^5J_{HH}$ 0.6; H^7), 7.62 m (H$^{6'}$), 7.51 td ($^3J_{HH}$ 7.3, $^5J_{HH}$ 1.2; H^5), 7.40 td ($^3J_{HH}$ 7.3, $^5J_{HH}$ 1.2; H^6), 7.30 m (H$^{3'}$), 7.19–7.12 m (2H$^{4', 5'}$); for {Pt(Dtc)}, 3.83 q ($^3J_{HH}$ 7.2; 2H$^{3''}$), 3.75 q ($^3J_{HH}$ 7.2; 2H$^{5''}$), 1.40 t ($^3J_{HH}$ 7.2; 3H$^{4''}$), 1.39 t ($^3J_{HH}$ 7.2; 3H$^{6''}$). ^{13}C{1H} NMR ($CDCl_3$; δ, ppm (*J*, Hz)): for {Pt(Pbt)}, 181.9 ($^2J_{Pt-C}$ 120.9; C^1), 151.1 (C^3), 146.0 ($^1J_{Pt-C}$ 1075.4; C$^{2'}$), 140.5 (C$^{1'}$), 132.4 ($^2J_{Pt-C}$ 85.2; C$^{3'}$), 131.8 ($^3J_{Pt-C}$ 62.4; C$^{4'}$), 131.4 (C^8), 127.5 (C^5), 125.4 (C^6), 125.0 (C$^{6'}$), 123.4 (C$^{5'}$), 122.4 (C^7), 120.3 (C^4); for {Pt(Dtc)}, 209.9 ($^3J_{Pt-C}$ 109.4; C$^{2''}$), 45.0 (C$^{3''}$), 44.8 (C$^{5''}$), 12.6 (C$^{4''}$), 12.5 (C$^{6''}$). ^{195}Pt NMR (CD_2Cl_2), δ, ppm: –3836.3.

O-Ethyldithiocarbonatobis((2-phenyl-3-ido)benzothiazole)iridium (**Ib**). ^{1}H NMR ($CDCl_3$), δ, ppm (*J*, Hz)): for {Ir(Pbt)$_2$}, 8.96 m (2H^4), 7.93 m (2H^7), 7.68 dd ($^3J_{HH}$ 7.7, $^4J_{HH}$ 1.0; 2H$^{6'}$), 7.51 ddd ($^3J_{HH}$ 7.8, 7.2, $^4J_{HH}$ 1.5; 2H^5), 7.47 ddd ($^3J_{HH}$ 7.4, 7.2, $^4J_{HH}$ 1.4; 2H^6), 6.88 td ($^3J_{HH}$ 7.6, $^4J_{HH}$ 1.0; 2H$^{5'}$), 6.68 ddd ($^3J_{HH}$ 7.7, 7.4, $^4J_{HH}$ 1.4; 2H$^{4'}$), 6.53 d ($^3J_{HH}$ 7.8; 2H$^{3'}$); for {Ir(Exn)}, 4.44 q ($^3J_{HH}$ 7.1; 2H$^{3''}$), 1.35 t ($^3J_{HH}$ 7.1; 3H$^{4''}$). ^{13}C{1H} NMR ($CDCl_3$; δ, ppm): for {Ir(Pbt)$_2$}, 180.3 (2C^1), 152.9 (2C^3), 150.8 (2C$^{2'}$), 140.9 (2C$^{1'}$), 133.7 (2C$^{3'}$), 131.8 (2C^8), 130.2 (C$^{5'}$), 127.1 (C^5), 125.8 (2C$^{6'}$), 125.3 (C^6), 122.5 (2C$^{4'}$, 2C^7), 121.6 (C^4); for {Ir(Exn)}, 230.0 (C$^{2''}$), 66.6 (C$^{3''}$), 13.8 (2C$^{4''}$).

O-Ethyldithiocarbonatobis((2-phenyl-3-ido)benzothiazole)platinum (**IIb**). ^{1}H NMR ($CDCl_3$; δ, ppm (*J*, Hz)): for {Pt(Pbt)}, 7.86 d ($^3J_{HH}$ 7.8; H^4), 7.84 d ($^3J_{HH}$ 6.4; H^7), 7.62 m (H$^{6'}$), 7.52 ddd ($^3J_{HH}$ 8.0, 7.3, $^4J_{HH}$ 0.7; H^5), 7.42 dd ($^3J_{HH}$ 8.0, 7.3; H^6), 7.27 m (H$^{3'}$), 7.17 m (2H$^{4'', 5''}$); for {Pt(Exn)}, 4.78 q ($^3J_{HH}$ 7.1; 2H$^{3''}$), 1.59 t ($^3J_{HH}$ 7.1; 3H$^{4''}$). ^{13}C{1H} NMR ($CDCl_3$), δ, ppm: for {Pt(Pbt)}, 181.9 (C^1), 150.6 (C^3), 143.7 (C$^{2'}$), 140.5 (C$^{1'}$), 133.3 (C$^{3'}$), 132.1 (C$^{4'}$), 131.2 (C^8), 127.7 (C^5), 125.7 (C^6), 125.2 (C$^{6'}$), 124.0 (C$^{5'}$), 122.6 (C^7), 120.4 (C^4); for {Pt(Exn)}, 246.6 (C$^{2''}$), 69.4 (C$^{3''}$), 13.9 (C$^{4''}$). ^{195}Pt NMR (CD_2Cl_2), δ, ppm: –4050.3.

The IR spectra of the complexes in KBr pellets were recorded on an IR Prestige-21 spectrometer of the Center for Collective Use at the Department of Chemistry of the Gertsen Russian State Pedagogical University. Electronic absorption and emission spectra were recorded on an SF-2000 spectrophotometer and a Flyuorat-02-Panorama spectrofluorimeter. Voltammograms were obtained on an ElinsPi-50-Pro system in a cell with divided spaces of the working (GC), auxiliary (Pt), and reference (Ag) electrodes in the presence of 0.1 M $[N(C_4H_9)_4]PF_6$ in a $C_6H_5CH_3$–CH_3CN (1 : 1) mixture. Peak potentials are presented at a rate of 100 mV/s with respect to a ferrocenium–ferrocene system.

RESULTS AND DISCUSSION

The X-ray diffraction analyses of complexes **Ia** and **IIb** (Fig. 1) show a distorted octahedral structure of iridium(III) complex **Ia** with the typical of biscycloiridated complexes [1] *cis*-C,C position of two equivalent metallated 2-phenylbenzothiazole ligands and a square structure of Pt(II) complex **IIb**. The donor S atoms of the chelating Exn^- and Dtc^- ligands form intramolecular hydrogen bonds C–H···S with the hydrogen atoms of the cyclometallated Pbt^- ligands (Fig. 1), namely, H(1) and H(5) in complex **IIb** and two H(12) atoms of the phenyl components of the Pbt^- ligands in complex **Ia**. Similarly to the earlier studied Ir(III) and Pt(II) complexes with metallated 2-phenylbenzothiazole [11–13], the M–N bond in structures **Ia** and **IIb** is longer than M–C by 0.08 and 0.08 Å, respectively (Table 2).

The *trans* position to the C atoms of the Pbt ligand in complex **Ia** results in an equivalence of two Ir–S bonds in the four-membered chelate {Ir(Dtc)}, whereas the square structure of complex **IIb** and the difference in the *trans* effect of the donor N and C atoms of the Pbt ligand induce the elongation of the Pt–S bond of the coordinated O-ethyldithiocarbonate ion (Table 2) by 0.16 Å in the *trans* position to the C atom compared to the *trans* position to the N atom. The formation of chelates {Ir(Dtc)} and {Pt(Exn)} results in an increase in the multiplicity of the C–N

Table 2. Bond lengths and bond angles in structures **Ia** and **IIb**

Bond	*d*, Å	Bond	*d*, Å
Ia		**IIb**	
Ir(1)–C(1)	2.022(13)	Pt(1)–C(1)	1.999(8)
Ir(1)–N(1)	2.097(9)	Pt(1)–N(1)	2.062(6)
Ir(1)–S(2)	2.469(3)	Pt(1)–S(2)	2.277(2)
		Pt(1)–S(3)	2.439(2)
C(14)–S(2)	1.727(12)	C(14)–S(3)	1.690(8)
		C(14)–S(2)	1.709(7)
C(14)–N(2)	1.390(2)	C(14)–O(2)	1.303(9)
Angle	ω, deg	Angle	ω, deg
S(2)Ir(1)S(2)	71.67(13)	S(2)Pt(1)(3)	74.24(6)
C(1)Ir(1)C(1)	93.4(7)	S(2)Pt(1)N(1)	107.96(17)
C(1)Ir(1)S(2)	97.5(4)	N(1)Pt(1)C(1)	80.6(3)
S(2)Ir(1)N(1)	88.8(4) 101.6(5)	C(1)Pt(1)S(3)	97.2(2)
C(1)IrN(1)	79.3(5) 91.9(5)		
Torsion angle	τ, deg		
N(1)C(1)Ir(1)S(2)	101.5(2)		

(**Ia**) and C–O (**IIb**) bonds with a decrease in their length by ~0.1 Å compared to the ordinary C–N (1.48 Å) and C–O (1.43 Å) bonds of the free Dtc^- and Exn^- ligands [14]. Similar C–N bond shortening due to an increase in its multiplicity was observed [15] for the cyclometallated complex [Pt(Bzq)Dmtc] (Bzq^- and $Dmtc^-$ are the deprotonated forms of benzo[h]quinoline and dimethyldithiocarbamate, respectively).

The results of IR spectroscopy for complexes **Ia**, **Ib**, **IIa**, and **IIb** (Table 3) are consistent with an increase in the multiplicity of the C–N and C–O bonds upon the coordination of the chelating ligands to Ir(III) and Pt(II). Compared to Na(Dtc), the C–N stretching vibration frequency is increased by 11 and 34 cm^{-1} for complexes **Ia** and **IIa**, respectively. An increase in the C–O stretching vibration frequency of O-ethyldithiocarbonate for the Ir(III) and Pt(II) complexes by 75 and 105 cm^{-1} compared to that in K(Exn) indicates a significant increase in the bond multiplicity of the Exn ligand in complexes **Ib** and **IIb**. The nonsplit C–S vibration frequency of the chelating Dtc and Exn ligands at 996 and 997 cm^{-1} corresponds to their bidentate coordination [16].

The data of ^1H NMR spectroscopy of the studied complexes show a similar *cis*-C,C structure of the Ir(III) octahedral complexes and a square structure of the Pt(II) complexes in a $CDCl_3$ solution and in the crystalline state. This is indicated by the magnetic equivalence of the H atoms of two cyclometallated ligands of the Ir(III) complex and a significant (by 0.9–1.0 ppm) upfield shift of the H(3') resonances of their phenyl protons (Table 4) due to the mutual anisotropic effect of circular currents of the phenyl components in the *cis* position. Unlike the Ir(III) complexes (**Ia**, **Ib**), the upfield shifts of the H(3') protons of the square Pt(II) complexes (**IIa**, **IIb**) are significantly lower: by 0.2–0.3 ppm. The overall upfield shift of the resonances of the phenyl protons of the Ir(III) and Pt(II) complexes shows an increase in the electron density of the phenyl component of the cyclometallated ligand. The different characters of shifts of the H(4') protons of the benzothiazole component of the cyclometallated ligands, namely, the downfield shift by 0.9–1.0 ppm for the Ir(III) complexes and the upfield shift by 0.2 ppm for the Pt(II) complexes, are consistent with the *trans*-N,N and *trans*-N,S positions of the donor atoms in the Ir(III) and Pt(II) complexes, respectively. The protons of the ethyl fragments of the Dtc and Exn ligands appear as quartets and triplets, respectively.

The selective 1D NOE experiment was carried out to refine the assignment of the H(3') proton in complex **Ib**. The observed nuclear Overhauser effect between the H(4) (9.44 ppm) and H(3') (6.59 ppm) protons of different cyclometallating ligands indicates that they are brought together in space.

The $^{13}C\{^1H\}$ NMR data for the complexes show (Table 4) that the metallation of 2-phenylbenzothiazole decreases the electron density of the C(1), C(1'), and C(2') atoms nearest to Ir(III) and Pt(II) in the complexes, which is manifested as a downfield shift of their signals by 4.5–24.1 ppm. The *trans* position of the donor S atoms of the Dtc and Exn ligands to the C atoms of the Pbt ligand in the Ir(III) complexes deter-

Table 3. Electronic and IR spectral and electrochemical parameters for complexes **Ia**, **Ib**, **IIa**, and **IIb***

Complex	Electronic spectra[a]			IR spectra[b]		Potential[c]	
	Absorption, λ_{max}, nm ($\varepsilon \times 10^3$ L mol^{-1} cm^{-1})	Emission, λ_{max}, nm (τ, μs)	Excitation, λ_{max}, nm	ν(CN/CO), cm^{-1}	ν(CS), cm^{-1}	Ox E_p, V[d]	Red -$E_{1/2}$, V
Ia	314 (37.6), 325 sh (30), 379 (7.83), 412 (6.74), 446 (5.02), 495 sh (2.8)	556, 600 sh, 675 sh (5.5)	382, 423, 442, 460 sh, 486	1488	986	0.66	2.20 2.49[d]
Ib	312 (36.8), 325 (35.3), 362 (10.8), 400 sh (7.8), 433 (6.37), 465 sh (4.9)	542, 18.45, 587 sh, 638 sh (6.0)	395, 425, 444, 465 sh, 485	1234	997	0.65	2.29[d] 2.47[d]
IIa	312 (17.0), 326 (16.2), 345 sh (8.2), 375 sh (6.7), 397 (11.4), 460 (1.92)	559, 601, 673 (5.6)	362, 396, 442, 455	1511	997	0.73	2.01
IIb	310 sh (14.8), 325 (16.7), 340 sh (14), 370 sh (7.8), 390 (11.7), 400 sh (7.6), 435 sh (2.3), 460 (3.06)	552, 595, 667 sh (5.4)	364 sh, 392, 427, 450, 460 sh	1262	997	0.32, 0.53, 0.74	2.08[d]

* a, CH_2Cl_2; b, KBr pellet; c, $C_6H_5CH_3$–CH_3CN (1 : 1); and d, current peak potential of the irreversible wave at the sweep rate 100 mV/s.

Table 4. Coordination-induced chemical shifts ($\delta_{comp} - \delta_{free\ ligand}$) of the H and C atoms of the ligands in the complexes*

Complex	$^1H^a$ {M(Pbt)}								$^1H^b$ {M(Dtc)}, {M(Exn)}			
	4	5	6	7	3'	4'	5'	6'	3''	4''	5''	6''
Ia	1.3	0.0	0.0	–0.2	–0.9	–0.8	–0.7	–0.4	–0.3	0.2	–0.2	0.1
Ib	0.9	0.0	0.0	–0.2	–1.0	–0.7	–0.6	–0.4	0.3	0.2		
IIa	–0.2	0.0	–0.1	–0.3	–0.3	–0.3	–0.4	–0.5	–0.2	0.2	0.1	–0.3
IIb	–0.2	0.0	–0.1	–0.3	–0.2	–0.2	–0.3	–0.5	0.3	0.2		

Complex	$^{13}C^a$ {M(Pbt)}												
	1	3	4	5	6	7	8	1'	2'	3'	4'	5'	6'
Ia	12.0	2.4	–0.5	–4.3	0.6	–0.9	–1.4	5.0	24.1	–4.0	–3.2	0.9	6.3
Ib	12.3	–1.1	0.1	–3.8	0.2	–0.6	–1.7	5.1	23.3	–3.1	–2.7	1.3	6.2
IIa	13.6	–2.9	–1.2	–3.4	0.3	–0.7	–1.7	4.5	18.5	–3.9	–2.8	2.9	4.9
IIb	13.9	–3.4	–1.1	–3.2	0.6	–0.5	–2.6	4.5	16.2	–3.7	–3.6	3.2	5.8

Complex	$^{13}C^b$ {M(Dtc)}, {M(Exn)}				
	2''	3''	4''	5''	6''
Ia	–5.8	–6.4	0.1	–6.4	0.1
Ib	–5.4	–8.3	–4.0		
IIa	2.8	–4.9	0.3	–4.6	0.2
IIb	11.2	–3.5	–2.4		

* a: with respect to HPbt in $CDCl_3$; b: with respect to Na(Dtc) or K(Exn) in D_2O.

mines the upfield shift of the resonances of the C(2") atoms of the chelating ligands by 5.4–5.8 ppm due to the enhancement of the electron density. At the same time, the square structure of the Pt(II) complexes results in the downfield shift of the resonance of the C(2") atom by 2.8 ppm for the diethyldithiocarbamate ion and by 11.2 ppm for the O-ethyldithiocarbonate ion, indicating an decrease in the electron density due to an efficient donor–acceptor interaction of the chelating ligands with Pt(II).

The enhanced efficiency of the donor–acceptor interaction of the O-ethyldithiocarbonate ligand with Pt(II) compared to diethyldithiocarbamate is confirmed by the upfield shift by 214 ppm of the resonance of the platinum atom in the ^{195}Pt NMR spectra of complex **IIb** compared to complex **IIa**.

In terms of the model of localized molecular orbitals [17], photo- and electrostimulated processes of complexes are conventionally classified depending on the predominant localization of the involved orbitals on the ligand and metal: ligand-centered, metal-centered, or the metal–ligand, ligand–metal, and ligand–ligand charge transfer. The electronic absorption spectra of the Ir(III) and Pt(II) complexes in the short-wavelength range ($\lambda < 330$ nm) contain intense ($\varepsilon > 10^4$ L mol^{-1} cm^{-1}) bands almost independent of the nature of the metal (Table 4) and chelating ligands. Two cyclometallated ligands in the internal sphere of the Ir(III) complexes compared to one cyclometallated ligand in the Pt(II) complex determine an approximately twofold increase in the molar absorption coefficient of the bands. This makes it possible to assign them to spin-allowed inner-ligand π–π^* optical transitions mainly localized on the cyclometallated ligands.

Similarly to [Pt(Bzq)(Dmtc)] [15], less intense (ε = (8.2–1.9) × 10^3 L mol^{-1} cm^{-1}) long-wavelength (λ = 345–460 nm) absorption bands of the Pt(II) complexes (Fig. 2) were attributed to the spin-allowed optical charge-transfer transition involving occupied mixed d_{Pt}/p(S) and unoccupied π^*(Pbt) orbitals predominantly localized on the cyclometallated ligand. The absorption spectra of the Ir(III) complex (Fig. 2) also contain longer-wavelength charge-transfer absorption bands (λ = 379–495 nm, $\varepsilon \approx 10^3$ L mol^{-1} cm^{-1}). However, the increased spin-orbital coupling constant of Ir(III) ($\varsigma \approx 5000$ cm^{-1} [18]) determines the conventional character of the division of optical transitions into spin-allowed and spin-forbidden transitions and overlap of absorption bands. Due to a lower efficiency of the interaction of the donor atoms of the S-chelating ligands with Ir(III) compared to Pt(II), the degree of mixing of the d_{Ir}/p(S) orbitals decreases, resulting in the predominant nature of the d_{Ir}–π^*(Pbt) OPTICAL bands of the Ir(III) complex.

If the Koopmans theorem [19] is valid for complexes **Ia**, **Ib**, **IIa**, and **IIb**, one can expect similarity between the orbitals of the complexes responsible for the long-wavelength optical transition and the character of their oxidation and reduction. Since the internal sphere of the Pt(II) and Ir(III) complexes contains one and two cyclometallated 2-phenylbenzothiazole ligands, respectively, the reduction voltammograms of the complexes are characterized by one and two one-electron waves, respectively (Fig. 3), which makes it possible to assign them to ligand-centered electron transfers to the π^* orbitals of cyclometallated 2-phenylbenzothiazole

$$[Pt(Pbt)(S\hat{}S)] + e^- \Leftrightarrow [Pt(Pbt^-)(S\hat{}S)]^-,$$

$$[Ir(Pbt)_2(S\hat{}S)] + e^- \Leftrightarrow [Ir(Pbt^-)(Pbt)(S\hat{}S)]^- + e^- \Rightarrow [Ir(Pbt^-)_2(S\hat{}S)]^{2-}.$$

The irreversible one-electron oxidation waves of complexes **Ia**, **Ib**, and **IIa** are observed [20] (Fig. 3) in the range (0.65–0.73 V) typical of the metal-centered process of the Ir(III) and Pt(II) complexes with cyclometallated 2-phenylbenzothiazole

$$[Ir^{III}(Pbt)_2(S\hat{}S)] - e^- \Rightarrow [Ir^{IV}(Pbt)_2(S\hat{}S)]^+,$$

$$[Pt^{II}(Pbt)(Dtc)] - e^- \Rightarrow [Pt^{III}(Pbt)(Dtc)]^+.$$

The oxidation voltammogram of the Pt(II) complex with the O-ethyldithiocarbonate ligand (Fig. 4) is characterized by the irreversible wave with a current peak maximum at 0.32 V and two additional low-intensity waves with maxima at 0.53 and 0.74 V. This is related, most likely, to the enhanced donor–acceptor interaction of the chelating ligand with Pt(II), resulting in an increase in the electron density of Pt(II) and the combined occurrence of the metal- and ligand-centered processes

$$[Pt^{II}(Pbt)(Exn)] - e^- \rightarrow [Pt^{III}(Pbt)(Exn)]^+$$

$$[Pt^{II}(Pbt)(Exn)] - e^- \rightarrow [Pt(Pbt)(Exn^+)]^+$$

The results of studying the electrochemical reduction and oxidation of the complexes are consistent with the d/p(S)–π^*(Pbt) nature of the long-wavelength charge-transfer bands in the absorption spectra of the complexes.

The photoexcitation of solutions of the complexes in the range of charge-transfer bands (Fig. 2) results in vibrationally structured phosphorescence in the yel-

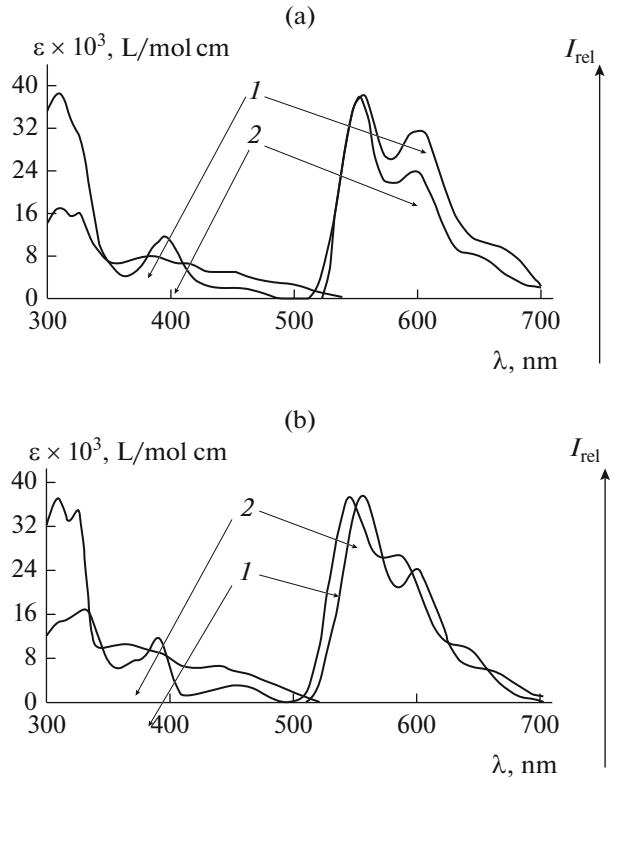

Fig. 2. Absorption and emission spectra of the complexes in a solution of CH_2Cl_2: (a) (*1*) [Pt(Pbt)(Dtc)] and (*2*) [Ir(Pbt)$_2$(Dtc)]; (b) (*1*) [Pt(Pbt)(Exn)] and (*2*) [Ir(Pbt)$_2$(Exn)].

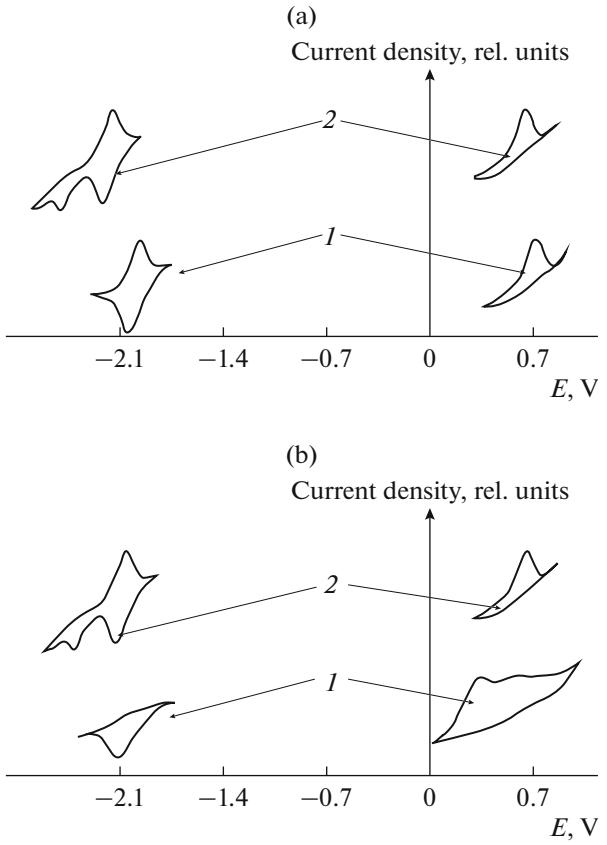

Fig. 3. Oxidation and reduction voltammograms for the complexes in a $C_6H_5CH_3$–CH_3CN (1 : 1) solution: (a) (*1*) Pt(Pbt)(Dtc)] and (*2*) [Ir(Pbt)$_2$(Dtc)]; (b) (*1*) [Pt(Pbt)(Exn)] and (*2*) [Ir(Pbt)$_2$(Exn)].

low-orange spectral range with the exponential decay kinetics τ = 5.4–6.0 μs. The phosphorescence excitation spectra are consistent with the absorption spectra (Table 4), which corresponds to the phosphorescence of the complexes due to the spin-forbidden *d/p*(S)–π*(Pbt) optical charge-transfer transition. The phosphorescence spectrum of the Pt(II) complex with the diethyldithiocarbamate chelating ligand is hypsochromically shifted by 100 cm^{-1} compared to the Ir(III) complex, whereas the enhanced interaction of the O-ethyldithiocarbonate ion with Pt(II) results in the bathochromic shift by 330 cm^{-1}.

The obtained results show that the optical and electrochemical properties of the cyclometallated octahedral Ir(III) complexes and the square Pt(II) complexes with diethyldithiocarbamate and O-ethyldithiocarbonate ions are determined by the predominant localization of the LUMO on the π* orbitals of metallated 2-phenylbenzothiazole and HOMO localization on the mixed *d/p*(S) orbital of the metal-chelating ligand. An increase in the degree of mixing of the *d* orbitals of Pt(II) with the S orbitals of the O-ethyldithiocarbonate ion results in the cathodic shift of the oxidation potential and in the bathochromic shift of the phosphorescence spectrum of the complex.

ACKNOWLEDGMENTS

This work was carried out in the framework of the state program of the Ministry of Education and Science of the Russian Federation (no. 4.131.2014K).

REFERENCES

1. Chi, Y. and Chou, P.T., *Chem. Soc. Rev*. 2010, vol. 39, no. 2, p. 638.
2. Fan, C. and Yang, C., *Chem. Soc. Rev.*, 2014, vol. 43, no. 17, p. 6439.
3. Goldsmith, G.I., Hudson, W.R., Lowry, M., et al., *J. Am. Chem. Soc.*, 2005, vol. 127, no. 20, p. 7502.
4. Rogers, C.W. and Wolf, M.O., *Coord. Chem. Rev.*, 2002, vols. 233–234, p. 341.
5. Yang, Y., Zhao, Q., Feng, W., et al., *Chem. Rev.*, 2013, vol. 113, no. 1, p. 192.
6. Zhao, J., Ji, S., Wu, W., et al., *Royal Soc. Chem. Adv.*, 2012, vol. 5, p. 1712.
7. Lamansky, S., Djurovich, P., Murphy, D., et al., *Inorg. Chem.*, 2001, vol. 40, no. 7, p. 1704.
8. Sheldrick, G.M., *Acta Crystallogr., Sect. A: Found. Crystallogr.*, 2008, vol. 64, no. 1, p. 112.

9. Dolomanov, O.V., Bourhis, L.J., Gildea, R.J., et al., *J. Appl. Crystallogr.*, 2009, vol. 42, no. 2, p. 339.

10. CrysAlisPro. Agilent Technologies. Version 1.171.36.20 (release 27-06-2012).

11. Katlenok, E.A., Zolotarev, A.A., and Balashev, K.P., *Russ. J. Coord. Chem.*, 2015, vol. 41, no. 1, p. 37.

12. Katlenok, E.A., Zolotarev, A.A., and Balashev, K.P., *Russ. J. Gen. Chem.*, 2015, vol. 85, no. 1, p. 116.

13. Katlenok, E.A., Zolotarev, A.A., and Balashev, K.P., *Russ. J. Gen. Chem*. 2014, vol. 84, no. 8, p. 1593.

14. *Kratkii spravochnik fiziko-khimicheskikh velichin* (Brief Handbook on Physiico-Chemical Quantities), Mishchenko, and K.P. Ravdelya, A.A., Eds., Leningrad: Khimiya, 1967.

15. Fornies, J., Sicilia, V., Casas, J.M., et al., *Dalton Trans.*, 2011, vol. 40, no. 12, p. 2898.

16. Awang, N., Baba, I., Yamin, B.M., et al., *Am. J. Appl. Sci*., 2011, vol. 8, no. 4, p. 310.

17. DeArmond, K., Hanck, K.W., and Wertz, D.W., *Coord. Chem. Rev.*, 1985, vol. 64, p. 65.

18. Montati, M., Credi, A., Prodi, L., and Gandolfi, T., *Handbook of Photochemistry,* Roca Ration: CRS /Talor & Francis, 2006, p. 617.

19. Koopmans, T., *Physics*, 1933, vol. 1, no. 1, p. 104.

20. Katlenok, E.A., Zolotarev, A.A., and Balashev, K.P., *Russ. J. Gen. Chem.*, 2015, vol. 85, no. 1, p. 116.

Translated by E. Yablonskaya